

**Table III.** Crystallographic Data for  $[\text{W}(\text{CO})_5\text{SnClFe}(\text{CO})_4]_2[\text{Na}_2((\text{C}_2\text{H}_5)_2\text{O})_4(\text{C}_4\text{H}_8\text{O}_2)]$  (1) at 130 K

chem formula	$\text{C}_{38}\text{H}_{48}\text{Cl}_2\text{Fe}_2\text{Na}_2\text{O}_{24}\text{Sn}_2\text{W}_2$
fw	1722.46
space group	$P\bar{1}$ (No. 2)
$a$ , Å	9.919 (2)
$b$ , Å	12.656 (3)
$c$ , Å	13.131 (4)
$\alpha$ , deg	67.72 (2)
$\beta$ , deg	77.65 (4)
$\gamma$ , deg	70.67 (2)
$V$ , Å <sup>3</sup>	1432.0 (6)
$D$ (calcd, 130 K), g/cm <sup>3</sup>	1.38
$Z$	1
radiation; $\lambda$ , Å	Mo K $\alpha$ ; 0.71069
$\mu$ (Mo K $\alpha$ ) cm <sup>-1</sup>	57.67
transmission factors	0.36-0.68
$R(F_o)$	0.057
$R_w(F_o)$	0.063

mm tubes and broad-band proton decoupling. An external  $\text{Sn}(\text{CH}_3)_4$  reference and the high frequency positive convention were used in reporting all chemical shifts. Infrared spectra were recorded in tetrahydrofuran solution on an IBM IR32 Fourier transform infrared spectrometer.

**Synthesis of  $[\text{W}(\text{CO})_5\text{SnClFe}(\text{CO})_4]_2[\text{Na}_2((\text{C}_2\text{H}_5)_2\text{O})_4(\text{C}_4\text{H}_8\text{O}_2)]$  (1).** Solid  $\text{Na}_2\text{Fe}(\text{CO})_4 \cdot 1.5\text{C}_4\text{H}_8\text{O}_2$  (1.24 g, 3.58 mmol) was added slowly to  $[\text{W}(\text{CO})_5\text{SnCl}_2(\text{OC}_4\text{H}_9)]$  (2.10 g, 3.58 mmol) in 30 mL of tetrahydrofuran at  $-78^\circ\text{C}$ . The reaction mixture progressively turned dark brown during the addition. The reaction mixture was allowed to come to room temperature and then stirred for an additional 1 h. At this point everything had dissolved to form a dark brown, opaque solution. The tetrahydrofuran was removed under vacuum, and the brown residue was redissolved in 40 mL of diethyl ether. Filtration of this solution through a bed of Celite and concentration to about 25 mL followed by slow cooling to  $-20^\circ\text{C}$  gave 1.22 g of brown crystals in 63% yield.

**X-ray Data Collection.** Brown plates were formed by slowly cooling (from  $+23$  to  $-20^\circ\text{C}$ ) a saturated diethyl ether solution of the compound. The crystals were removed from the Schlenk tube under a stream of dry nitrogen and quickly covered with a light hydrocarbon oil (Exxon Paratone N) to protect them from the atmosphere. The crystal was mounted on a glass fiber and secured in the nitrogen cold stream of a  $P_21$  diffractometer equipped with a locally modified LT-1 low-temperature apparatus and a graphite monochromator. Data were collected at 130 K. Unit cell parameters were obtained from a least-squares refinement of 10 reflections with  $17 < 2\theta < 26^\circ$ . The crystal lattice was found to be triclinic  $P$  by the automatic indexing routine of the software available on the diffractometer; no symmetry was observed in any of the axial photographs. A unique hemisphere of data was collected to a  $2\theta_{\text{max}}$  of  $50^\circ\text{C}$ , yielding 5531 data. A total of 4514 data with  $I > 3\sigma(I)$  were used in the solution and refinement of the structure. No decay in the intensities of two standard reflections occurred. Crystal parameters are summarized in Table III. The data were corrected for Lorentz and polarization effects.

**Solution and Refinement of Structure.** The positions of tin, tungsten, and iron were generated by FMAP 8, the Patterson-solving routine of SHELXTL, version 5. Other atom positions were located from successive difference Fourier maps. Anisotropic thermal parameters were assigned to the tin, tungsten, iron, sodium, and chlorine atoms. Isotropic thermal parameters were used for the remaining atoms. Hydrogen atoms were placed at idealized positions ( $d(\text{C}-\text{H}) = 0.96 \text{ \AA}$ ) and assigned isotropic thermal parameters 20% greater than the carbon atom to which they were attached. They were refined by using a riding model. A correction for absorption was applied.<sup>16</sup> Neutral-atom scattering factors were those of Cromer and Waber.<sup>17</sup> The largest feature on the final difference Fourier map was  $2.8 \text{ e/\AA}^3$ . This peak was  $1.01 \text{ \AA}$  from the tungsten atom.

**Acknowledgment.** We thank the National Science Foundation (Grant CHE-8519557) for support.

**Registry No.** 1, 116887-72-0;  $[\text{W}(\text{CO})_5\text{SnCl}_2(\text{OC}_4\text{H}_9)]$ , 65198-59-6;  $\text{Na}_2\text{Fe}(\text{CO})_4 \cdot 1.5\text{C}_4\text{H}_8\text{O}_2$ , 59733-73-2; Fe, 7439-89-6; Sn, 7440-31-5; W, 7440-33-7.

- (16) XABS produces an absorption tensor from an expression relating  $F_o$  and  $F_c$ ; Moezzi, B. Ph.D. Thesis University of California, Davis, CA, 1988.  
 (17) *International Tables for X-ray Crystallography*; Kynoch: Birmingham, England, 1974; Vol. 14, pp 149-150, 99-101.

**Supplementary Material Available:** Listings of all bond lengths, bond angles, hydrogen atom positions, anisotropic thermal parameters, and data collection parameters and three views of structural elements (8 pages); a listing of observed and calculated structure factors (27 pages). Ordering information is given on any current masthead page.

Contribution from the Institute of Inorganic and Applied Chemistry, University of Hamburg, D-2000 Hamburg 13, FRG

### Interaction of Vanadate ( $\text{H}_2\text{VO}_4^-$ ) with Dipeptides Investigated by $^{51}\text{V}$ NMR Spectroscopy

Dieter Rehder

Received February 24, 1988

Vanadium is rapidly attaining the status of a widely spread biometal in both its oxidation states V (where it is present, at physiological pH, in the form of dihydrogen orthovanadate and several condensed species<sup>1</sup>) and IV/III. Two enzymes containing vanadium as an essential metal have been discovered recently: (i) a vanadate(V)-dependent haloperoxidase present in marine brown and red algae<sup>2,3</sup> and in a lichen<sup>4</sup> and (ii) nitrogenases isolated from specific strains of *Azotobacter vinelandii* and *Azotobacter chroococcum*, which contain vanadium instead of molybdenum.<sup>5</sup> The importance of vanadium in nitrogen fixation has in fact been documented already more than a half-century ago.<sup>6</sup> Further, the chemical similarity between inorganic phosphate and vanadate has prompted a number of investigations into the possible antagonism between these two anions in bioreactions<sup>7</sup> ever since the discovery of the inhibitory action of vanadate toward the sodium-potassium pump.<sup>8</sup> Both inhibitory and stimulating functions of vanadate have been documented,<sup>9</sup> which makes this anion also interesting in medication and in toxicological studies. In most if not all of its actions, vanadate is or becomes an integral part of a large protein molecule. Despite a few investigations concerned with the coordination of V(V), V(IV), and V(III) to serum transferrin<sup>10,11</sup> and the interaction of vanadate(V) with ribo-

- (1) (a) Pettersson, L.; Hedman, B.; Andersson, I.; Ingri, N. *Chem. Scr.* **1983**, *22*, 254. (b) Pettersson, L.; Andersson, I.; Hedman, B. *Chem. Scr.* **1985**, *25*, 309. (c) Pettersson, L.; Hedman, B.; Nenner, A.-M.; Andersson, I. *Acta Chem. Scand., Ser. A* **1985**, *A39*, 499. (d) Ivakin, A. A.; Kurbatova, L. D.; Kruchinina, M. V.; Medvedeva, N. I. *Russ. J. Inorg. Chem. (Engl. Transl.)* **1986**, *31*, 219. In this communication, a trinuclear species,  $\text{V}_3\text{O}_{10}^{5-}$ , and its monoprotonated form are described in addition to the vanadates reported by Pettersson et al.  
 (2) (a) Vilter, H. *Phytochemistry* **1984**, *23*, 1387. (b) de Boer, E.; van Kooyk, Y.; Tromp, M. G. M.; Plat, H.; Wever, R. *Biochim. Biophys. Acta* **1986**, *869*, 48.  
 (3) Krenn, B. E.; Plat, H.; Wever, R. *Biochim. Biophys. Acta* **1987**, *912*, 287.  
 (4) Plat, H.; Krenn, B. E.; Wever, R. *Biochem. J.* **1987**, *248*, 277.  
 (5) (a) Robson, R. L.; Eady, R. R.; Richardson, T. H.; Miller, R. W.; Hawkins, M.; Postgate, J. R. *Nature (London)* **1986**, *322*, 388. (b) Arber, M. J.; Dobson, B. R.; Eady, R. R.; Stevens, P.; Hasnain, S. S.; Garner, C. D.; Smith, B. E. *Nature (London)* **1987**, *325*, 372.  
 (6) Bortels, H. *Zentralbl. Bakteriol.* **1936/37**, *95*, 13.  
 (7) Gresser, M. J.; Tracey, A. S.; Stankiewicz, P. *J. Adv. Protein Phosphatases* **1987**, *4*, 35.  
 (8) Cantley, L. D., Jr.; Josephson, L.; Warner, R.; Yanagisawa, M.; Lechene, C.; Guidotti, G. *J. Biol. Chem.* **1977**, *252*, 7421.  
 (9) For a comprehensive account see: Chasteen, N. D. *Struct. Bonding (Berlin)* **1983**, *53*, 105.  
 (10) Butler, A.; Danzitz, M. J. *J. Am. Chem. Soc.* **1987**, *109*, 1864. There are arguments against the assignment of the signals observed at  $-530$  ppm to transferrin-bound vanadate: In a large molecule containing a quadrupolar nucleus, the long molecular correlation time should give rise to signals of at least several kilohertz in width. We feel that the rather sharp signals described in this communication are due to complex formation of vanadate with small fragments of transferrin.  
 (11) (a) Chasteen, N. D.; Grady, J. K.; Holloway, C. E. *Inorg. Chem.* **1986**, *25*, 2754. (b) Bertini, I.; Canti, G.; Luchinat, C. *Inorg. Chim. Acta* **1982**, *67*, L21.

Table I.  $^{51}\text{V}$  NMR Data<sup>a</sup> for Vanadate Solutions (10 mmol/L, pH 7.5 (2)) Containing Amino Acids and Dipeptides

ligand	c(ligand), mmol/L	V-ligand complex			$T_1$ $\delta$	$T_2^b$ $\delta$	$T_4$		$T_5^{c,d}$ $\delta$
		$\delta$	$I^e$	$W_{1/2}$			$\delta$	$I^e$	
Tris <sup>f</sup>	100	-528, -542 <sup>g</sup>			-558	-572	-577	8.3	-585
gly	600				-556	vw	-574	15	-581
asp	600				-554	vw	-573	8.6	-580
ser	600	-536, <sup>h</sup> -552 sh			-555	-570	-575	4.2	-584
gly-asp	17	-507	0.7		-555	-570	-575	4.6	-583
	35	-510	1.7	320	-556	-572	-577	3.8	-586
	75	-508	4.6	450	-555	-570	-575	2.9	-583
	100	-508	5.6	420	-556	-571	-575	3.6	-583
	125	-507	7.2	410	-557	-571	-575	2.7	-585
	200	-509	10	410	-557	-572	-577	3.7	-585
	250	-507	13	510	-555	-571	-575	2.8	-583
	300	-509	14	440	-557	-572	-576	3.0	-584
	400	-509	22	500	-557	-572	-576	2.0	-584
	600	-509	25	510	-556	-572	-576	0.6	-584
gly-gly	600	-504	15	360	-557	-572	-576	3.0	-584
gly-tyr	90	-509	11	780	-557	-572	-577	1.5	-585
gly-ser	115	-493	1.0						
		-506	6.5	420	-555	-571	-575	1.5	
	300	-494	3.0	490					
		-507	21	480	-556		-576	2.3	-583
gly-glu	115	-505	3.6	520	-554	-570	-574	2.6	-584
Z-gly-glu	300	<i>i</i>			-558	-572	-576		-585
Z-glu-tyr	100				-550 <sup>j</sup>	-568	-574	4.6	-583
val-asp	115				-556	-570	-575	10	-583
pro-gly	100	-493	9.9	450	-559	-573	-577	2.1	-585
gly-pro	110				-559	-573	-577	5.8	-585
gly-sar	100				-558	-572	-577	6.7	-585

<sup>a</sup> Bruker AM 360 at 94.73 MHz and 298 (1) K, 10 mm diameter vials, 2/1 H<sub>2</sub>O/D<sub>2</sub>O; sweep width 100 kHz, 16K data set, pulse angle 60°, line-broadening factor 10–15 Hz, 1000–6000 scans; standard VOCl<sub>3</sub> in CDCl<sub>3</sub>, all  $\delta$  values corrected for lock shift. <sup>b</sup> Relative intensity 0.4–0.8. <sup>c</sup> Relative intensity 0.1–0.4. <sup>d</sup> In many cases, there are one or two additional, very weak signals at -587 ( $T_6$ ) and -596 ppm (broad; unassigned). <sup>e</sup> Integral intensity relative to H<sub>2</sub>T<sub>1</sub> = 1. <sup>f</sup> Tris is the tris(hydroxymethyl)aminomethane/HCl buffer, 0.2 M (see also ref 13a and 27b). <sup>g</sup> Very broad signal. <sup>h</sup> Weak and broad signal. <sup>i</sup> A weak signal at -514 ppm is probably due to an impurity in the peptide. <sup>j</sup> Very broad; cf. Figure 1b.

nuclease A<sup>12</sup> and peroxidases,<sup>2,13</sup> only little is known about the coordination environment of vanadium in the protein matrix.

In order to model potential binding sites, we have investigated the complexation of vanadate by dipeptides. Preliminary results and also basic aspects of the background theory for the interpretation of  $^{51}\text{V}$  NMR spectra have been included in a recent communication.<sup>14</sup> In the present work, a number of simple dipeptides, in many cases containing glycine at the N-terminal end, have been selected with respect to the elucidation of their mode of coordination. Several aspects of the complex formation are exemplified with an acidic amino acid, viz. H-gly-asp-OH as a constituent of the peptide. Acidic side chains of the protein matrix are likely involved in vanadate coordination in vanadate-dependent peroxidase.<sup>13</sup> The nucleus  $^{51}\text{V}$  (nuclear spin  $7/2$ , natural abundance 99.75%, relative receptivity ( $^1\text{H} = 1$ ) 0.38) belongs to the low-quadrupole category (quadrupole moment  $-0.052 \times 10^{-28} \text{ m}^2$ ) and is a particularly convenient nucleus in NMR experiments for this reason, which provides information from quadrupole relaxation and satisfactory spectral resolution due to reasonably narrow resonance signals.<sup>15</sup>

At pH values around 7.5 and at low overall vanadium concentrations (10 mmol/L), the species present in solution are

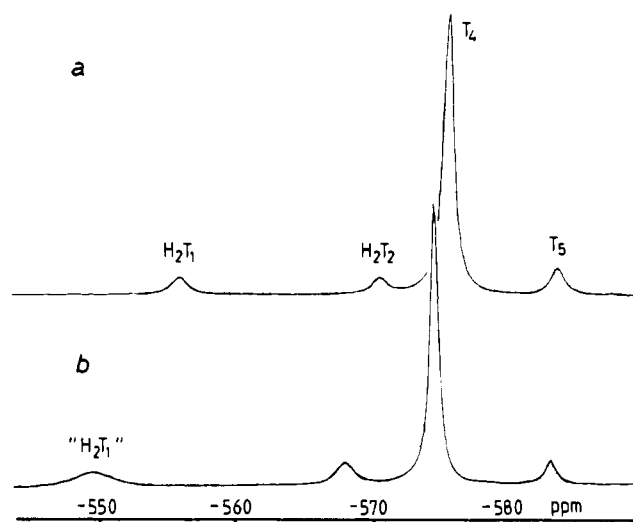
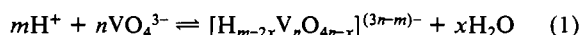


Figure 1.  $^{51}\text{V}$  NMR spectra of vanadate (10 mmol/L) and H-val-asp-OH (115 mmol/L) at pH 7.6 (a) and Z-glu-tyr-OH (100 mmol/L) at pH 7.6 (b). The upper spectrum shows the distribution of the four main vanadate species in a system, where no complexation occurs; the bottom spectrum illustrates the involvement of vanadate in weak complexation by a broadening and low-field shift mainly of the diprotonated mono-vanadate. The line width and shift parameters of the signal indicated "H<sub>2</sub>T<sub>1</sub>" reflect the equilibrium position of two species, H<sub>2</sub>T<sub>1</sub> and a vanadate-peptide complex, in comparatively rapid exchange.

H<sub>2</sub>VO<sub>4</sub><sup>-</sup> (H<sub>2</sub>T<sub>1</sub>; pK<sub>a</sub> = 7.92), H<sub>2</sub>V<sub>2</sub>O<sub>7</sub><sup>2-</sup> (H<sub>2</sub>T<sub>2</sub>; pK<sub>a</sub> = 8.02), V<sub>4</sub>O<sub>12</sub><sup>4-</sup> (T<sub>4</sub>), and V<sub>5</sub>O<sub>15</sub><sup>5-</sup> (T<sub>5</sub>), and possibly also V<sub>6</sub>O<sub>18</sub><sup>6-</sup> (T<sub>6</sub>), with T<sub>4</sub> being the dominating species.<sup>1</sup> The shifts  $\delta(^{51}\text{V})$ , quoted relative to VOCl<sub>3</sub>, are contained in Table I. Figure 1a gives an approximate visual impression of the distribution of the various specimens. Protonation and nucleation equilibria, which can be summarized as shown in eq 1,<sup>16</sup> are of potential importance in



- (12) Borah, B.; Chen, C.-W.; Egan, W.; Miller, M.; Wlodawer, A.; Cohen, J. S. *Biochemistry* **1985**, *24*, 2058. In this paper, the reference signal (H<sub>2</sub>VO<sub>4</sub><sup>-</sup>) is incorrectly assigned. The correct  $\delta(^{51}\text{V})$  for the resonance of the reported vanadate-uridine complex is -523 relative to VOCl<sub>3</sub>.
- (13) (a) Vilter, H.; Rehder, D. *Inorg. Chim. Acta* **1987**, *136*, L7. (b) Rehder, D.; Vilter, H.; Duch, A.; Priebsch, W.; Weidemann, C. *Recl. J. R. Neth. Chem. Soc.* **1987**, *106*, 408. (c) Hormes, J.; Kuetgens, U.; Chauvistre, R.; Schreiber, W.; Anders, N.; Vilter, H.; Rehder, D.; Weidemann, C. *Biochim. Biophys. Acta*, in press.
- (14) Rehder, D.; Weidemann, C.; Duch, A.; Priebsch, W. *Inorg. Chem.* **1988**, *27*, 584. In this communication, we have suggested coordination of the dipeptides via the peptide N and the carboxylate group. In the light of the more detailed investigations presented in this work, other coordination modes are likely.
- (15) (a) Rehder, D. *Bull. Magn. Reson.* **1982**, *4*, 33. (b) Rehder, D. *Magn. Reson. Rev.* **1984**, *9*, 125. (c) Rehder, D. In *Multinuclear NMR*; Mason, J., Ed.; Plenum: New York, 1987; Chapter 19.

**Table II.** Effects of pH<sup>a</sup> and Vanadate Concentration<sup>b</sup> on the System Vanadate/H-gly-asp-OH

pH	c(V), <sup>c</sup> mM	V-ligand complex <sup>d</sup>		T <sub>1</sub> <sup>e</sup>		T <sub>2</sub> δ	I(T <sub>4</sub> ) <sup>f,g</sup>
		I <sup>f</sup>	[complex], <sup>h</sup> mM	δ	[T <sub>1</sub> ], <sup>h</sup> mM		
6.85	10.0	7.9	5.9	-560	0.75	-573	2.8
7.39	10.0	7.0	5.4	-557	0.78	-572	2.9
7.54	10.0	5.1	4.9	-556	0.95	-571	3.0
8.13	10.0	3.4	4.2	-552	1.23	-571	2.8
8.38	10.0	1.7	2.9	-548	1.71	-569	2.7
8.52	10.0	1.0	2.0	-546	2.01	-569	2.4
7.46	1.65	6.9	1.4	-557	0.21		
7.44	3.3	6.4	2.9	-557	0.43	w	
7.35	6.7	6.1	5.2	-558	0.85	-572	0.4
7.41	10.0	6.1	6.1	-557	1.00	-571	2.7
7.43	13.3	6.3	8.9	-558	1.41	-573	1.7
7.43	16.7	6.6	9.9	-558	1.50	-572	2.6
7.35	20.0	6.3	10.8	-558	1.71	-572	3.2
7.39	28.7	6.6	11.8	-559	1.79	-573	6.3

<sup>a</sup>pH/D, in 2/1 H<sub>2</sub>O/D<sub>2</sub>O. Peptide concentration 110 mM. <sup>b</sup>Peptide concentration 125 mM. <sup>c</sup>Total vanadate concentration. <sup>d</sup>δ values for the complex -509 (1) ppm and W<sub>1/2</sub> values 410 (15) Hz throughout. <sup>e</sup>Limiting values for the T<sub>1</sub> species are -560 (H<sub>2</sub>T<sub>1</sub>) and -537 ppm (HT<sub>1</sub>).<sup>1a</sup> <sup>f</sup>I is the intensity relative to T<sub>1</sub> = 1. <sup>g</sup>δ values -576 (1) ppm throughout. Also present is the T<sub>3</sub> species (-585 ppm). See also footnote d in Table I. <sup>h</sup>Equilibrium concentration, by <sup>51</sup>V NMR.

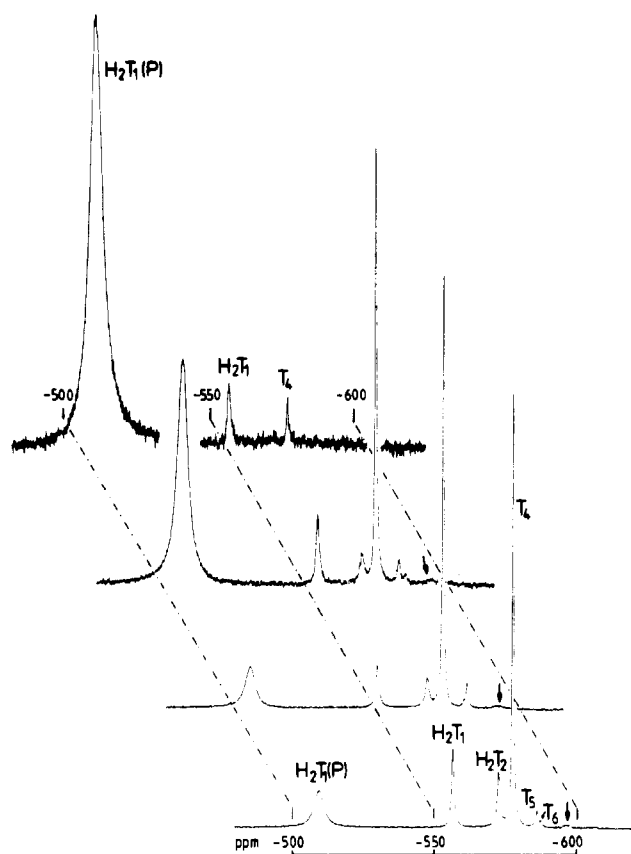


**Figure 2.** Spectra of vanadate (10 mmol/L) and H-gly-asp-OH in varying molar ratios  $c(\text{peptide})/c(\text{V})$  (bottom to top) 3.5/1, 7.5/1, 20/1, and 60/1; pH 7.4–7.7. The high-field signal indicated by an arrow is not assigned. H<sub>2</sub>T<sub>1</sub>(P) is the peptide–vanadate complex, the formation of which is practically completed as the peptide concentration becomes 600 mmol/L. See also Table I for additional information.

addition to equilibria involving the complexation of a peptide ligand. The interchange between H<sub>2</sub>T<sub>1</sub> and H<sub>2</sub>T<sub>2</sub> is comparatively fast; the equilibria involving the polynucleated anions T<sub>4</sub>, T<sub>5</sub>, and T<sub>6</sub> are slow (cf. ref 16).

The <sup>51</sup>V NMR results of the interaction between vanadate, the amino acids glycine, serine, and aspartic acid, and various dipeptides are summarized in Tables I and II. Illustrative spectra

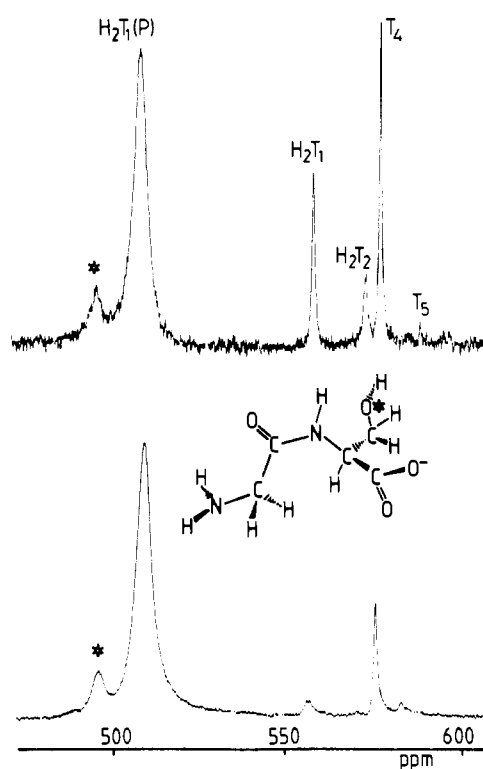


**Figure 3.** <sup>51</sup>V NMR spectra of vanadate (10 mmol/L) plus H-gly-ser-OH, pH 7.5, at 115 mmol/L (above) and 300 mmol/L. The asterisk denotes involvement of the hydroxy group of the serine moiety in coordination.

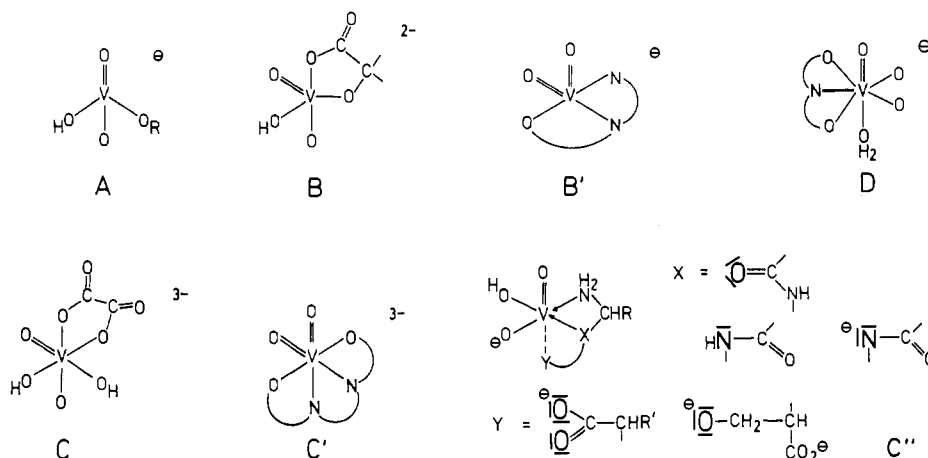
are given in Figures 1–3. Complex formation is indicated by a signal at ca. -505 ppm. The resonance is relatively broad (widths at half-height typically are 420 Hz), and this is not unexpected for quadrupole-dominated relaxation in a molecule containing a sterically demanding ligand and with the vanadium nucleus at a low-symmetry site.<sup>15</sup> In the case of the amino acids glycine and aspartic acid, even a 60-fold excess of the potential ligand does not provide any vanadate species containing the carboxylato ligand, and these findings contrast with investigations carried out by Pettersson et al. on the vanadate–oxalate system<sup>17</sup> and by Gresser and Tracey on oxalate, lactate, and glycerate.<sup>18</sup> There is an indication for some interaction with serine; the signal positions

(16) Tytko, K. H.; Mehmke, J. Z. *Anorg. Allg. Chem.* **1983**, *503*, 67. The β values (β = log K; K is the formation constant) are 28.4 for H<sub>2</sub>T<sub>1</sub> and 41.3 for T<sub>4</sub>. The β values reported in ref 1b are 18.7 and 43.2, respectively, based on H<sub>2</sub>T<sub>1</sub>.

(17) Ehde, P. M.; Andersson, I.; Pettersson, L. *Acta Chem. Scand., Ser. A* **1986**, *A40*, 489.

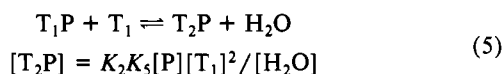
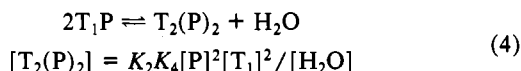
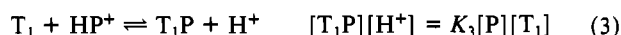
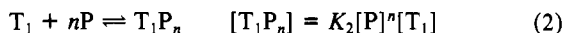
(18) Tracey, A. S.; Gresser, M. J.; Parkinson, K. M. *Inorg. Chem.* **1987**, *26*, 629.

Chart I



are, however, different from the typical peptide resonance. Dipeptides carrying an N-terminal protective group (Z-gly-tyr-OH and Z-gly-glu-OH; Z is the carbobenzoxy substituent) do not show the resonance typical of vanadate-peptide interaction, but in the case of Z-gly-tyr-OH, the downfield shift and broadening of the  $T_1$  resonance (Figure 1b) is indicative of rapid exchange between  $H_2T_1$  and a labile complex (possibly a peptide complex with a coordination of the peptide different from what will be discussed below for peptides with an available  $NH_2$ ), with the equilibrium position close to uncomplexed monovanadate. A broadening of the resonance line for monovanadate, although not to this extent, is observed quite generally in our samples, while the oligovanadates are not affected.

Equations 2–5 describe complexation equilibria which might be considered ( $H_2NCH(R)C(O)NHCH(R')CO_2^- \equiv P$ ;  $n = 1$  in eq 3–5; see the discussion below). We have investigated the



equilibrium conditions for the interaction of vanadate with H-gly-asp-OH (H-gly-asp-O<sup>-</sup> at pH 7.5), for which complex formation increases as the pH decreases (Table II). A protonated species is therefore involved, and the only one present in significant amounts is  $H_2T_1$ . From the data in Table II is obtained a straight line for the plot of  $[H_2T_1P]$  vs  $[H_2T_1]$  in the pH range 6.85–8.52; i.e., we can exclude a  $[H^+]$ -dependent complexation equilibrium (eq 3). If dinuclear complexes are formed, as has been observed with, e.g., lactate,<sup>18</sup>  $[H_2T_1]$  should be proportional to the square root of the equilibrium concentration of the complex (eq 4 and 5). However, this is not the case: A plot of [complex] vs  $[H_2T_1]$  for constant peptide and variable vanadate concentrations (see the data given in Table II) indicates a *linear* relationship and therefore a mononuclear vanadate-peptide complex. From the slope  $K_2[P]^n = 6.1$  and a peptide concentration of  $0.125 \text{ mol}\cdot\text{L}^{-1}$ ,  $K_2^{1/n} = 49 \text{ L}\cdot\text{mol}^{-1}$ . From the *linear* correlation [complex]/ $[H_2T_1]$  vs  $[P]$  for constant overall vanadate and varying peptide concentrations (data from Table I),  $K_2 = 49$ . Hence,  $n = 1$  (eq 2). There is no indication for the formation of a 1:2 complex in the concentration range considered ( $c(P) = 17\text{--}300 \text{ mmol}\cdot\text{L}^{-1}$ ). It has been suggested by Crans et al.<sup>19</sup> that the intensity ratio of the signals for the complex and monovanadate be employed as a measure of the relative complex stability. With the data in Table I (and for a concentration ratio  $c(P)/c(V) \approx 10$ ), the rang of the

dipeptides in a series of increasing ability to coordinate to vanadate is H-val-asp-OH  $\approx$  H-gly-pro-OH  $\ll$  H-gly-glu-OH  $<$  H-gly-asp-OH  $\approx$  H-gly-ser-OH  $<$  H-pro-gly-OH  $<$  H-gly-tyr-OH.

An interesting special case is the complexes that are formed with H-gly-ser-OH (Figure 3). Two signals at  $-494$  and  $-507$  ppm in the approximate intensity ratio 1:7 are observed. While the signal at  $-507$  is the "normal" one also observed with other dipeptides, the lower intensity signal at  $-494$  ppm is new and apparently has to be assigned to a complex where the alcoholic function of the serine takes part in coordination to vanadium. Other serine-containing peptides exhibit the same low-field component. Serine itself does not show this resonance but a weak and broad component centered at  $-539$  ppm plus a low-field shoulder of the  $H_2T_1$  resonance at ca.  $-555$  ppm. The signal at  $-539$  ppm is at the same position as one of the strong resonances that have been reported for the vanadate-lactate system under similar conditions, for which an octahedral coordination had been proposed.<sup>18</sup>

Vanadium(V) has a versatile coordination geometry (Chart I), and coordination numbers ranging between 4 and 7 have been reported and verified by X-ray analyses.<sup>20</sup> Among the functions principally available for interaction with the vanadate anion, the carboxylate should be, at first sight, a likely candidate, as established, inter alia, for oxalate,<sup>21a-c</sup> picolinate, and dipicolinate,<sup>21d,e</sup> and also for the edta ligand,<sup>22</sup> which have been shown to constitute octahedral and pentagonal-bipyramidal complexes (C, C', and D in Chart I). For lactate and glycerate, the coordination number 5 has been deduced and a trigonal-bipyramidal structure has been proposed<sup>18</sup> (B), but the tetragonal pyramid has also been found for the coordination number 5, e.g. in the azine complex B'.<sup>23</sup> Ligands containing alcoholic functions form acyclic esters of tetrahedral geometry<sup>24</sup> or, if there are two vicinal OH groups present, cyclic esters corresponding to the constitution B in Chart I.<sup>25</sup>

For the vanadate-peptide complexes, it seems not unreasonable to assume octahedral geometry (C''), which has also been found for the edta complex (C'). Since amino acids do not coordinate

- (20) Compounds formerly reported to exhibit the coordination number 8 (e.g.  $V(O_2)_3ox^{3-}$ ; ox is the oxalato(2-) ligand) have more recently been shown to be 7-coordinated complexes of the composition  $VO(O_2)_2ox^{3-}\cdot H_2O_2$ : Campbell, L. J.; Capparelli, M. V.; Griffith, W. P.; Skapski, A. C. *Inorg. Chim. Acta* **1983**, *77*, L215.
- (21) (a) Scheidt, W. R.; Tsai, C.; Hoard, J. L. *J. Am. Chem. Soc.* **1971**, *93*, 3867. (b) Yamada, S.; Katayama, C.; Tanaka, J.; Tanaka, M. *Inorg. Chem.* **1984**, *23*, 253. (c) Stomberg, R. *Acta Chem. Scand.; Ser. A* **1986**, *A40*, 168. (d) Szentivanyi, H.; Stomberg, R. *Acta Chem. Scand.; Ser. A* **1983**, *A37*, 709. (e) Drew, R. E.; Einstein, F. W. B. *Inorg. Chem.* **1973**, *12*, 229.
- (22) Scheidt, W. R.; Collins, D. M.; Hoard, J. L. *J. Am. Chem. Soc.* **1971**, *93*, 3873.
- (23) Petrović, A. F.; Ribár, B.; Petrović, D. M.; Leovac, V. M.; Gerbeleu, N. V. *J. Coord. Chem.* **1982**, *11*, 239.
- (24) Gresser, M. J.; Tracey, A. S. *J. Am. Chem. Soc.* **1985**, *107*, 4215.
- (25) Gresser, M. J.; Tracey, A. S. *J. Am. Chem. Soc.* **1986**, *108*, 1935.

the vanadate to a sizable extent, the peptide group attains a key position, and chelate formation through the additional use of the amino and/or carboxylate groups is likely to occur. Since N-protected dipeptides and also H-val-asp-OH (with a sterically demanding isopropyl group in the vicinity of the amino function) do not coordinate, the N-terminal end appears to participate. Considering the peptide linkage, potential candidates for vanadate coordination are the carbonyl oxygen and the amide nitrogen. Although the lone pair of the latter takes part in double bonding to the adjacent carbonyl carbon, there are strong arguments for its involvement in complex formation, arising from the observation that H-gly-pro-OH and H-gly-sar-OH (with a tertiary amide function in the peptide linkage) do not undergo complex formation.

In conclusion, we have shown, using  $^{51}\text{V}$  NMR spectroscopy, that vanadate forms complexes with dipeptides at physiological pH, which may model vanadium binding sites in proteins. The complexes that are mononuclear at least in the case of H-gly-asp-OH, although comparatively weak, are stronger by 1-2 orders of magnitude than those which have been documented with oxalate and lactate.<sup>18</sup> The peptide function and the N-terminal amino group are involved in coordination (C' in Chart 1), but appropriate side-chain functions of the C-terminal amino acid, such as a hydroxyl group, may also participate. The low-field shift of the  $^{51}\text{V}$  resonance relative to the vanadates and also relative to various complexes with hydroxy carboxylates<sup>18,26</sup> is in accord with at least one nitrogen in the first coordination sphere.<sup>14,15</sup> Similar downfield shifts have been reported for the vanadate complexes formed with tris(hydroxymethyl)aminomethane<sup>27</sup> and several derivatives of ethanolamine,<sup>19</sup> for which N-O coordination has been proposed.

**Acknowledgment.** This work was supported by the Deutsche Forschungsgemeinschaft.

**Registry No.** gly, 56-40-6; asp, 56-84-8; ser, 56-45-1; Z-gly-glu, 3916-39-0; Z-gly-tyr, 988-75-0; val-asp, 20556-16-5; gly-pro, 704-15-4; gly-sar, 29816-01-1;  $\text{H}_2\text{VO}_4^-$ , 34786-97-5;  $\text{H}_2\text{V}_2\text{O}_7^{2-}$ , 103884-11-3;  $\text{V}_4\text{O}_{12}^{4-}$ , 12379-27-0;  $\text{V}_5\text{O}_{15}^{5-}$ , 78197-82-7; V, 7440-62-2.

(26) Caldeira, M. M.; Ramos, M. L.; Oliveira, N. C.; Gil, V. M. S. *Can. J. Chem.* **1987**, *65*, 2434.

(27) Tracey, A. S.; Gresser, M. J. *Inorg. Chem.*, in press.

Contribution from the Department of Chemistry and Biochemistry, Texas Tech University, Lubbock, Texas 79409

### Displacement of Carbon-Bonded Chloranilate from the $[\text{Pd}(\text{C-CA})\text{Cl}_2]^{2-}$ Ion by Hydrochloric Acid

Woo-Yeong Jeong and Robert A. Holwerda\*

Received May 26, 1988

Although the susceptibility of alkylpalladium(II) compounds toward decomposition in acidic media is well documented,<sup>1-6</sup> kinetic studies of palladium-carbon bond cleavage induced by hydrogen ion have not been carried out. We recently initiated

- (1) Carturan, G.; Graziani, M.; Ros, R.; Belluco, U. *J. Chem. Soc., Dalton Trans.* **1972**, 262.
- (2) Ito, T.; Tsuchiya, H.; Yamamoto, A. *Bull. Chem. Soc. Jpn.* **1977**, *50*, 1319.
- (3) Coronas, J. M.; Sales, J. J. *Organomet. Chem.* **1975**, *94*, 107.
- (4) Ceder, R.; Granel, J.; Muller, G.; Rossell, O.; Sales, J. J. *Organomet. Chem.* **1979**, *174*, 115.
- (5) Diversi, P.; Ingrassio, G.; Lucherini, A. *J. Chem. Soc., Chem. Commun.* **1978**, 735.
- (6) Roe, D. M.; Bailey, P. M.; Moseley, K.; Maitlis, P. M. *J. Chem. Soc., Chem. Commun.* **1972**, 1273.

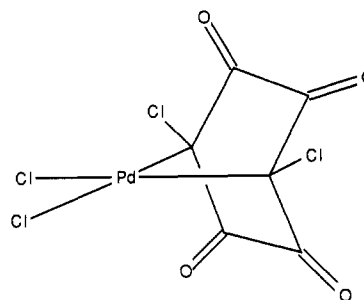
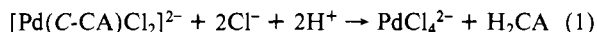


**Figure 1.** Structure of the  $[\text{Pd}(\text{C-CA})\text{Cl}_2]^{2-}$  ion in  $\text{K}_2[\text{Pd}(\text{CA})\text{Cl}_2] \cdot 4\text{H}_2\text{O}$ , adapted from ref 8. Pd-C bond lengths are 2.02 and 2.07 Å, and the bend angle of chloranilate in the boat conformation is 46.0°.

synthetic and mechanistic studies of palladium(II) compounds with hydroxyquinone ligands in order to systematically examine the dynamics of Pd-C bond-making and bond-breaking reactions in systems that do not exhibit complicating side reactions such as mixed alkane/olefin generation coupled with partial reduction of Pd(II) to Pd(0).<sup>7</sup> Thus, the dichloro(chloranilato)palladate(II) ion, originally prepared and structurally characterized by Krasochka et al.,<sup>8</sup> contains chloranilate ( $\text{CA}^{2-}$ ) bonded as a bent, bis(carbanion) donor (Figure 1) rather than as a conventional  $\pi$ -complex ( $\pi\text{-CA}^{2-}$ ) of the quinonoid 2,5-dioxo-3,6-dichloro-1,4-benzoquinone resonance form. We previously reported that carbon-bonded chloranilate ( $\text{C-CA}^{2-}$ ) in  $[\text{Pd}(\text{C-CA})\text{Cl}_2]^{2-}$  is retained upon the extraction of chloride ion by  $\text{AgNO}_3$  in acetonitrile to give  $[\text{Pd}(\text{C-CA})(\text{CH}_3\text{CN})_2]$ , which accepts triphenylphosphine readily with accompanying linkage isomerization, generating  $[\text{Pd}(\pi\text{-CA})(\text{PPh}_3)_2]$ .<sup>7</sup>

During the investigation of  $\text{K}_2[\text{Pd}(\text{C-CA})\text{Cl}_2]$  as a precursor to other (chloranilato)palladium(II) compounds, it was noted that the complex slowly decomposes in aqueous HCl, affording  $\text{PdCl}_4^{2-}$  and unionized chloranilic acid ( $\text{H}_2\text{CA}$ ) as the sole products (eq 1). In contrast, the complex loses chloride and ultimately decays



to palladium metal in neutral or basic aqueous solutions that do not contain excess chloride ion. As part of our continuing mechanistic studies of Pd-C bond cleavage reactions, we report here kinetic measurements on the protonolysis reaction (1) at 50 °C. Of particular interest is the question of whether both the incoming nucleophile and electrophile participate in the rate-determining step.

### Experimental Section

$\text{K}_2[\text{Pd}(\text{C-CA})\text{Cl}_2] \cdot 0.5\text{H}_2\text{O}$  was prepared and characterized as previously described.<sup>7</sup> Standardized HCl and  $\text{HClO}_4$  solutions were used in conjunction with NaCl to determine the hydrogen and chloride ion dependences of observed pseudo-first-order protonolysis rate constants ( $k_{\text{obsd}}$ ) at a constant ionic strength of 1.0 M. Decay of freshly prepared  $[\text{Pd}(\text{C-CA})\text{Cl}_2]^{2-}$  solutions (50  $\mu\text{M}$ ) in a 1 cm path length cell thermostated at  $50.0 \pm 0.2$  °C was monitored by using the 260-nm absorbance decrease (Perkin-Elmer Lambda 5 spectrophotometer) associated with reaction 1. Reported  $k_{\text{obsd}}$  values, derived from the linear least-squares slopes of  $\ln(A_t - A_\infty)$  vs time plots, are the average of at least five trials.

### Results and Discussion

In acidic chloride media, the release of carbon-bonded chloranilate from  $[\text{Pd}(\text{C-CA})\text{Cl}_2]^{2-}$  proceeds quantitatively according to the stoichiometry of eq 1. Ultraviolet peaks of the reactant<sup>7</sup> at 236 nm ( $\epsilon 2.2 \times 10^4 \text{ M}^{-1} \text{ cm}^{-1}$ ), 264 nm ( $\epsilon 1.8 \times 10^4 \text{ M}^{-1} \text{ cm}^{-1}$ ), and 312 nm ( $\epsilon 1.5 \times 10^4 \text{ M}^{-1} \text{ cm}^{-1}$ ) are replaced by the intense 222- and 300-nm bands characteristic of  $\text{PdCl}_4^{2-}$  and  $\text{H}_2\text{CA}$ , respectively, with four well-defined isosbestic points at 234, 280, 311, and 430 nm. Considering these isosbestic points and the fact that the equilibrium UV spectrum agrees well with that calculated from the sum of  $\text{PdCl}_4^{2-}$  and  $\text{H}_2\text{CA}$  absorbances, it may be

(7) Jeong, W.-Y.; Holwerda, R. A. *Inorg. Chem.* **1988**, *27*, 2571.

(8) Krasochka, O. N.; Avilov, V. A.; Atovmyan, L. O. *Zh. Strukt. Khim.* **1974**, *15*, 1140.